Precuneus Degeneration in Nondemented Elderly Individuals With *APOE* ε4: Evidence From Structural and Functional MRI Analyses

Yaojing Chen,[1,2] Zhen Liu,[1,2] Junying Zhang,[1,2] Kewei Chen,[2,3] Li Yao,[1,4] Xin Li,[1,2] Gaolang Gong,[1,2] Jun Wang,[1,2]* and Zhanjun Zhang[1,2]*

[1]*State Key Laboratory of Cognitive Neuroscience and Learning & IDG/McGovern Institute for Brain Research, Beijing Normal University, Beijing, People's Republic of China*
[2]*BABRI Centre, Beijing Normal University, Beijing, People's Republic of China*
[3]*Banner Alzheimer's Institute, Phoenix, Arizona*
[4]*Information Processing Lab, College of Information Science and Technology, Beijing Normal University, Beijing, People's Republic of China*

Abstract: Neurodegenerative diseases such as Alzheimer's disease (AD) have been recognized to exhibit disease-specific brain vulnerability patterns. Apolipoprotein E (*APOE*) ε4 allele imparts a high genetic risk of developing AD. Whether the *APOE* ε4 allele damages the brain when cognitive functions are still intact is important to understand, especially for possible early detection and intervention. This study aimed to examine the selective degeneration pattern associated with the *APOE* ε4 allele in the brains of cognitively normal elderly subjects. We enrolled 35 cognitively healthy ε4 carriers and 40 non-carriers (53 to 81 years old) to evaluate group differences in cortical thickness and brain activation during a memory-encoding task. We also assessed the functional connectivity of the brain regions with both structural and functional damages. The results from the neuropsychological tests showed that the performances of ε4 carriers and non-carriers were comparable. Primarily, we found that the precuneus exhibited thinner cortical thickness and decreased deactivation during memory encoding. Furthermore, the connectivity analyses show that carriers exhibited damaged connectivity of the precuneus to several regions in the default mode network and the attention/executive control network. Our study reveals the degeneration pattern of the ε4 allele, which could be used as a potential biomarker for early detection for possible interventions and treatments. *Hum Brain Mapp 38:271–282, 2017.*

Key words: Alzheimer's disease; APOE ε4 allele; cortical thickness; deactivation; functional connectivity; precuneus

The first two authors equally contributed to this work.
Contract grant sponsor: State Key Program of National Natural Science of China; Contract grant number: 81430100; Contract grant sponsor: Natural Science Foundation of China; Contract grant number: 30873458, 81173460; Contract grant sponsor: Beijing New Medical Discipline Based Group; Contract grant number: 100270569; Contract grant sponsor: Beijing Municipal Science & Technology Commission; Contract grant number: Z161100000216135; Contract grant sponsor: National Institute on Aging; Contract grant number: R01AG031581 and P30AG19610; Contract grant sponsor: International Cooperation and Exchange of the National Natural Science Foundation of China; Contract grant number: 61210001

*Correspondence to: Zhanjun Zhang, MD, State Key Laboratory of Cognitive Neuroscience and Learning, and BABRI Centre, Beijing Normal University, Beijing 100875, China. E-mail: zhang_rzs@bnu.edu.cn and Jun Wang, PhD, State Key Laboratory of Cognitive Neuroscience and Learning, and BABRI Centre, Beijing Normal University, Beijing 100875, China. E-mail: jun_wang@bnu.edu.cn

Received for publication 13 April 2016; Revised 16 August 2016; Accepted 16 August 2016.
DOI: 10.1002/hbm.23359
Published online 4 September 2016 in Wiley Online Library (wileyonlinelibrary.com).

INTRODUCTION

Alzheimer's disease (AD) is a severe neurodegenerative disease characterized by progressive cognitive decline [Ferri et al., 2005]. Several studies have suggested that the initial brain degeneration caused by AD is selective in nature, i.e., the pathological alterations in the brain emerge from a limited number of vulnerable brain regions that can be structurally or functionally networked [Buckner et al., 2009; Murray et al., 2011]. Supporting the view of this selective degeneration process, several studies have revealed the influence of regional atrophy in specific brain structures on functional networks in AD [La Joie et al., 2014; Zhou et al., 2012], such as the default mode network (DMN) and consequent episodic memory dysfunction [Buckner et al., 2005; Seeley et al., 2009]. Furthermore, evidence from amyloid pathology, one of the hallmark pathologies of AD, has indicated that the DMN is preferentially degenerated due to amyloid retention in AD [Klunk et al., 2004]. The selective degeneration concept synthesizes both structural and functional dynamic changes in AD as a way to comprehend neural pathological lesions starting before the onset of the disease, i.e., in the preclinical phase of the disease.

The apolipoprotein E (*APOE*) ε4 allele is the best known genetic risk factor of late-onset AD [Coon et al., 2007]. People who possess the *APOE* ε4 allele have an early onset age [Reinvang et al., 2013]. The relationship between *APOE* ε4 and specific degeneration patterns in cognitively normal elderly individuals is unknown. As for episodic memory, the *APOE* ε4 carriers, those without dementia at baseline, showed a faster decline in task performance during 6 years of clinical evaluations [Barnes et al., 2013]. With regard to brain structure and function, *APOE* ε4 was associated with significant impairments long before the onset of AD in cognitively normal people [Reinvang et al., 2013]. Separately, *APOE* ε4 carriers were shown to accelerate brain atrophy rates before the onset of cognitive impairments in middle-aged persons [Chen et al., 2007] and in elderly subjects [Donix et al., 2010]. Even in healthy children and adolescents, the *APOE* ε4 allele causes thinning of the cortex in the left entorhinal region [Shaw et al., 2007]. Additionally, increased activation in the medial temporal lobe was observed in healthy older ε4 carriers during an episodic memory task [Nichols et al., 2012], which was similar to AD patients during repeated stimuli in the same regions [Pihlajamaki et al., 2008]. In addition, several studies on cognitively normal elderly people demonstrate that the ε4 allele disrupts brain network connectivity, including connectivity of both the posterior [Damoiseaux et al., 2012; Machulda, 2011; Sheline et al., 2010a] and the anterior [Damoiseaux et al., 2012] DMNs and the salience network [Sheline et al., 2010a]. In middle-aged cognitively healthy adults, the connectivity of the DMN and the executive control network are also decreased in the ε4 carriers compared with non-carriers [Goveas et al., 2013].

These persuasive and consistent findings have highlighted the need for a systematic examination to clarify the existence of a possible selective degeneration pattern in people who are cognitively normal but who have an increased risk of AD due to carrying the ε4 allele. If such a degeneration phenotype was identified in the preclinical stages, it may help clinicians understand the disease onset characteristics and better plan AD prevention and early treatment trials despite the absence of longitudinal studies to verify these findings.

Specifically, we hypothesized that the *APOE* ε4 allele first leads to selective degeneration in specific regions structurally and/or functionally in the preclinical stage and that such degeneration affects functional integration throughout the brain regions. We first examined the atrophy of selective regions induced by the ε4 allele in cognitively normal elderly people. Second, we determined brain efficiency during a memory-encoding task and investigated whether the task-dependent activation variations were affected by the relevant structural abnormalities. Finally, we considered the functional connectivity (FC) of the targeted brain region through the structural impairment and memory-encoding activation deficits.

Abbreviations

ACC	Anterior cingulate cortex
ANCOVA	Analysis of covariance
APOE	Apolipoprotein E
BABRI	Beijing Aging Brain Rejuvenation Initiative
DMN	Default mode network
FC	Functional connectivity
fMRI	Functional MRI
ICV	Intracranial volume
MCI	Mild cognitive impairments
MFG	Middle frontal gyrus
MMSE	Mini-mental status examination
MPFC	Medial prefrontal cortex
MP-RAGE	Magnetization prepared rapid gradient echo
MRI	Magnetic resonance imaging
PCC	Posterior cingulate cortex
PV	Partial volume
RFT	Random field theory
SFG	Superior frontal gyrus
STG	Superior temporal gyrus
TE	Echo time
TR	Repetition time

MATERIALS AND METHODS

Participants

Data from a total of 75 right-handed, native Chinese participants were used in this study [Chen et al., 2015]. The data were obtained from the Beijing Aging Brain Rejuvenation Initiative (BABRI) database. The Ethics Committee and institutional review board of Beijing Normal University's Imaging Centre for Brain Research approved

TABLE I. Demographic and neuropsychological characteristics of *APOE* ε4 carriers and non-carriers

	APOE ε4 Carriers ($n = 35$)	*APOE* ε4 Non-carriers ($n = 40$)	F/T-value (X^2)	P-value
Age (years)	67.26 ± 1.29	64.45 ± 1.15	1.63	0.11[a]
Male/Female	17/18	19/21	0.01	1.00[b]
Education (years)	11.31 ± 0.54	10.75 ± 0.49	0.77	0.44[a]
General mental status				
MMSE	27.11 ± 0.33	27.30 ± 0.24	0.01	0.93
Memory function				
AVLT-delay recall	4.23 ± 0.50	3.68 ± 0.41	0.42	0.52
AVLT-T	26.06 ± 1.88	23.98 ± 1.41	0.19	0.66
ROCF-delay recall	11.11 ± 1.15	10.53 ± 1.08	0.01	0.92
Backward digit span	4.45 ± 0.27	3.87 ± 0.20	2.54	0.12
Digit span	12.09 ± 0.52	10.85 ± 0.31	1.96	0.17
Visuo-spatial processing				
ROCF-Copy	33.06 ± 0.64	32.83 ± 0.43	0.61	0.44
CDT	24.80 ± 0.67	23.55 ± 0.60	0.13	0.72
Language				
CVFT	43.51 ± 1.82	40.23 ± 1.27	1.52	0.22
BNT	23.71 ± 0.66	23.38 ± 0.64	0.01	0.94
Attention				
SDMT	31.83 ± 1.98	33.08 ± 1.77	0.37	0.55
SCWT-B Time (s)	41.77 ± 1.74	39.68 ± 1.11	0.52	0.47
TMT-A time (s)	64.71 ± 5.79	55.56 ± 3.98	1.06	0.31
Executive function				
SCWT C-B Time (s)	43.26 ± 3.15	42.85 ± 4.22	0.70	0.41
TMT-B time (s)	191.57 ± 12.47	177.58 ± 10.61	2.68	0.11
Episodic memory task				
Encoding accuracy (%)	93.00 ± 3	95.54 ± 3	1.45	0.24
Encoding RT (msec)	1079.13 ± 64.60	1058.09 ± 39.27	0.05	0.82
Recognition accuracy (%)	77.33 ± 5	81.67 ± 4	1.33	0.26
Recognition RT (msec)	1036.50 ± 94.32	1004.15 ± 46.27	0.12	0.73

Values are mean ± S.E.M. or Nos. of participants.
The comparison of neuropsychological scores, episodic memory accuracy and reaction time between the two groups was performed with an analysis of covariance. MMSE = Mini-Mental Status Examination; AVLT = Auditory Verbal Learning Test; ROCF = Rey-Osterrieth Complex Figure test; CDT = Clock-Drawing Test; CVFT = Category Verbal Fluency Test; BNT = Boston Naming Test; SDMT = Symbol Digit Modalities Test; SCWT = Stroop Color and Word Test; TMT = Trail Making Test.
[a]The P value for age and education were obtained using an independent two-sample t-test.
[b]The P value for sex was obtained using a Chi-square test.

this study, and all participants gave written informed consent. To be included in this study, a subject had to meet the following criteria: (1) score of at least 24 on the Mini-Mental Status Examination (MMSE); (2) no history of neurologic, psychiatric, or systemic illnesses known to influence cerebral function, including serious vascular diseases, head trauma, tumour, current depression, alcoholism, and epilepsy; (3) no prior history of taking psychoactive medications; (4) able to cope with the physical demands of the magnetic resonance imager; and (5) Clinical Dementia Rating of 0. The following exclusion criteria were used in this study: (1) structural abnormalities other than cerebrovascular lesions, such as tumours, subdural haematomas, and contusions due to previous head trauma, that could impair cognitive function; (2) history of addictions, neurologic or psychiatric diseases, or treatments that would affect cognitive function; (3) large vessel disease, such as cortical or subcortical infarcts and watershed infarcts; and (4) diseases with white matter lesions, such as normal-pressure hydrocephalus and multiple sclerosis.

Neuropsychological Testing

All participants underwent a battery of neuropsychological tests that assessed their general mental status and other cognitive domains, such as memory, attention, spatial processing, executive function and language ability; the tests have been described in detail previously [Chen et al., 2014]. Thirteen neurocognitive measures were derived from 10 separate neuropsychological tests (Table I).

Analysis of Genotyping

Participants were pre-screened for the *APOE* genotype using a TaqMan SNP genotyping assay on a 7900HT Fast Real-Time PCR system (Applied Biosystems, Foster City,

USA). DNA was extracted from the blood samples of subjects for the subsequent characterization of the *APOE* genotype via PCR according to standard procedures. All participants were genotyped for two SNPs in the *APOE* gene (rs429358 and rs7412) using previously published methods [Felsky et al., 2012]. Genotype identifications were manually and independently verified by two laboratory personnel. Ten percent of sample genotypes underwent quality control duplication. There were 35 *APOE* ε4 carriers (including 32 subjects with an ε3/ε4 genotype and 3 subjects with an ε4/ε4 genotype) and 40 *APOE* ε4 non-carriers (including 30 subjects with an ε3/ε3 genotype and 10 subjects with an ε2/ε3 genotype) included in our present study.

Experimental Paradigm

The episodic memory task has a blocked periodic design and has been described in detail previously [Wang et al., 2013]. It consisted of an encoding task with two conditions (encoding and fixation) and a recognition task during the functional magnetic resonance imaging (MRI) acquisition. The task started with a 12-second presentation of a fixation cross. Then, four encoding blocks of 40 seconds were interleaved with four fixation blocks of 24 seconds. There were 10 trials per encoding block, of which five were natural and five were artificial (i.e., manmade) stimuli (each picture lasted 3.5 seconds followed by a fixation cross for 0.5 seconds) in two runs per subject. The participants were instructed to indicate their response by pressing the button on the MRI-compatible response box in their left or right hand (left, natural stimuli; right, artificial stimuli). For the fixation condition, a white cross on a black background was presented for the entire trial, and no response was required during this test. Recognition accuracy was assessed using a recognition task immediately after the encoding run. Subjects saw 40 pictures presented in random order, of which 20 pictures were previously shown during the encoding runs and the other 20 were new. Subjects were instructed to indicate whether the picture had been shown previously by pressing the button on the response box in either their left or right hand (left, yes; right, no). To make sure that each participant understood the instructions and performed the task correctly, they were asked to practice for 10–15 minutes before the experiment.

MRI Data Acquisition

All participants were scanned with a SIEMENS TRIO 3T scanner in the Imaging Center for Brain Research at Beijing Normal University, and high-resolution T1-weighted structural MRIs, episodic memory tasks and resting state functional scans were obtained. Participants laid supine with their heads fixed snugly by straps and foam pads to minimize head movement. T1-weighted, sagittal 3D magnetization prepared rapid gradient echo (MP-RAGE) sequences were acquired and covered the entire brain [176 sagittal slices, repetition time (TR) = 1900 ms, echo time (TE) = 3.44 ms, slice thickness = 1 mm, flip angle = 9°, inversion time = 900 ms, field of view (FOV) = 256 × 256 mm^2, acquisition matrix = 256 × 256]. Functional images were collected using an echo-planar imaging sequence that consisted of a TE = 30 ms, TR = 2000 ms, flip angle = 90°, 33 axial slices, slice thickness = 3.5 mm, acquisition matrix = 64 × 64, FOV = 200 × 200 mm^2. During the single-run resting acquisition, subjects were instructed to stay awake, relax with their eyes closed and remain as motionless as possible. The resting acquisition lasted for 8 minutes, and 240 image volumes were obtained. For episodic memory task imaging, each of the two functional runs had 221 volumes.

Structural Image Processing: Vertex-Based Morphology

We used the CIVET pipeline to measure the thickness and surface area on the cortical surface as previously described [Gong et al., 2012]. Briefly, the native T1-weighted magnetic resonance images were first linearly aligned into the stereotaxic space and corrected for non-uniformity artefacts using the N3 algorithm [Sled et al., 1998]. This algorithm does not require prior knowledge of the brain tissue classes and can iteratively estimate both the multiplicative bias field and the distribution of true tissue intensities for the automatic correction of intensity non-uniformity in MRI data. The resultant brain images were then automatically segmented into gray matter, white matter, cerebrospinal fluid, and background by using a partial volume (PV) classification algorithm, in which a trimmed minimum covariance determinant method was applied to estimate the parameters of the PV effect model; the parameter, β, controlling the relative strength of the Markov random field was set to 0.1 [Tohka et al., 2004]. Next, the inner and outer gray matter surfaces were automatically extracted for each hemisphere using the CLASP algorithm [Kim et al., 2005]. The individual surfaces were further aligned with a surface template to allow for comparisons across subjects at corresponding vertices. Cortical thickness was measured between the two surfaces at 40,962 vertices per hemisphere using the linked distance in the native space [Lerch and Evans, 2005]. The middle cortical surface, defined at the geometric centre between the inner and outer cortical surfaces, was used to calculate the cortical surface area in the native space [Lyttelton et al., 2009]. The thickness/surface area map was further blurred with a 30 mm surface-based diffusion smoothing kernel [Chung et al., 2003]. These methods have been validated using both manual measurements [Kabani et al., 2001] and a population simulation [Lerch and Evans, 2005] and have been widely applied.

We assessed the group differences in cortical thickness at each vertex. Specifically, a GLM with "group" as a predictor variable was applied, in which age, gender, education and intracranial volume (ICV) were included as covariates. To correct for multiple comparisons, a random field theory (RFT) based method was applied at the cluster-level [Taylor and Adler, 2003], and cortical clusters surviving an FWE-corrected $P < 0.05$ were considered significant. All statistical procedures were implemented using SurfStat (http://www.math.mcgill.ca/keith/surfstat/).

Functional Data Preprocessing

Functional data were preprocessed, and statistical analyses were performed using an SPM5 package (http://www.fil.ion.ucl.ac.uk/spm/software/spm5). Preprocessing procedures included slice timing, within-subject interscan realignment to correct for possible movement, spatial normalization to a standard brain template in the Montreal Neurological Institute coordinate space, resampling to $3 \times 3 \times 3$ mm^3, and smoothing with an 8 mm full-width half-maximum Gaussian kernel. Finally, the task functional data were high-pass filtered with a cutoff frequency of 0.01 Hz, whereas resting functional imaging data were processed with linear detrending and 0.01–0.08 Hz band-pass filtering.

Memory-Encoding Task Functional Data Analysis

In the single-subject level, data were analysed according to the fixed effects model (SPM5). The 6 head movement parameters were included in the model as confounding factors. Contrast images for encoding minus fixation were calculated. We considered the deactivated regions (i.e., those more active during fixation than encoding), which were assumed to constitute the DMN [McKiernan et al., 2003], during the episodic memory task. At the group level, one-sample t tests were further performed to characterize the DMN for the carrier and non-carrier groups separately. Statistical images were analysed using a corrected threshold of $P < 0.05$ (AlphaSim-corrected) to generate significant deactivation in each group. Therefore, we obtained the sum of regions mask based on significantly deactivated voxels in two groups for subsequent analyses. Finally, deactivation differences between groups were computed by a two-sample t-test using an inclusive regions mask. An AlphaSim-corrected threshold of $P < 0.05$ was identified as significantly activated.

Resting-State Data: Functional Connectivity Analysis With the Identified Atrophic Region as the Seed ROI

We selected seed locations based on the peaks of the group cortical morphology differences as spheres centred at each coordinate with a 6 mm radius. For each subject, time series in each ROI were obtained by averaging the functional MRI (fMRI) time series across all voxels over the given ROI. To regress out the nuisance covariates, time series were corrected for the patient movement, the global mean signal, the white matter signal and the cerebrospinal fluid signal. Pearson's correlation coefficient between the seed ROI signal time course and that of every voxel in the brain was computed. Prior to group comparisons, the correlation coefficients were converted to z-scores using the Fischer r-to-z transformation. Regions that have positive z-scores between two fluctuating time-courses indicate "in-phase" connections and the regions with negative z-scores indicate "out-of-phase" connections. These z-score images were entered into the statistical analysis.

For each group, one-sample t tests were further performed to generate significant positive and negative connectivity images (FDR-corrected, $q < 0.05$). Therefore, a conjunction analysis was used to identify the positive and negative regions common to both groups for subsequent analyses. We then used a two-sample t test to investigate between-group positive and negative connectivity differences in the common positive and negative masks (AlphaSim-corrected, $P < 0.05$).

Statistical Analysis

The Hardy-Weinberg test was completed using PLINK software [Purcell et al., 2007]. Independent two-sample t-tests were used to assess between-group differences in age and education. A chi-square test was used to compare gender ratio differences. For neuropsychological assessment, an analysis of covariance (ANCOVA) was used to test between-group differences (age, gender and education were included as covariates).

RESULTS

Demographic and Neuropsychological Measurements

A total of 75 cognitively normal elderly subjects participated in this study and were pre-screened for the *APOE* genotype and then split into two groups: *APOE* ε4 carriers and non-carriers. The demographic characteristics and neuropsychological test scores of the ε4 carrier and non-carrier groups are shown in Table I. No differences in age, gender, or education were found between carriers and non-carriers. After controlling for the effects of age, gender, and education, there were no statistically significant group differences in any neuropsychological measures, response times or accuracies during the episodic memory task.

APOE ε4 and Cortical Thickness

Cortical thickness was analysed to find the cortical thickness differences in carriers and non-carriers. For the

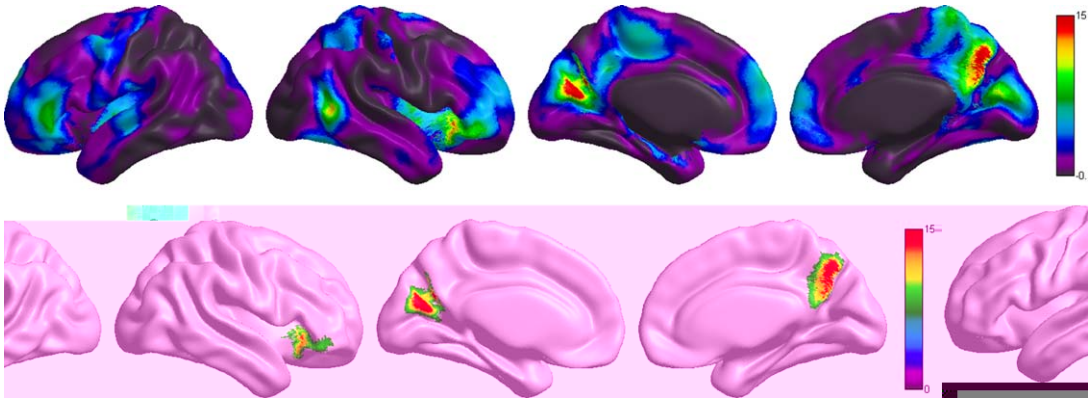

Figure 1.
The effect of the *APOE* ε4 genotype on cortical thickness. The *F* statistic map for the *APOE* ε4 genotype effect across the entire cerebral cortex. The significant cluster (FWE-corrected, $P < 0.05$) after the RFT based correction.

mean thickness of the entire cortical cortex, a significant group difference was observed ($F = 4.43$, $P = 0.039$). The vertex-based F map for the group effect on the thickness is illustrated in Figure 1. After RTF-based correction for multiple comparisons, three cortical clusters were significantly less thick in carriers (Fig. 1); the clusters were located on the left calcarine (mean cluster thickness: 3.34 ± 0.15 mm in carriers and 3.50 ± 0.16 mm in non-carriers), the right precuneus (PreCu.R, mean cluster thickness: 2.89 ± 0.14 mm in carriers and 3.03 ± 0.15 mm in non-carriers) and the right inferior frontal gyrus (IFG.R, mean cluster thickness: 3.67 ± 0.22 mm in carriers and 3.84 ± 0.17 mm in non-carriers) (FWE-corrected, $P < 0.05$). The regions of difference are also indicated in Table II.

APOE ε4 Effects on Regions During Tasks

In each group, contrasting the encoding condition with the fixation condition revealed consistency in the deactivated brain regions; these areas included the medial prefrontal cortex (MPFC), anterior cingulate cortex (ACC), precuneus/posterior cingulate cortex (PreCu/PCC), and angular gyrus, which comprised the DMN (Fig. 2a). Both groups exhibited activation in regions such as the inferior frontal gyrus, precentral gyrus, postcentral gyrus, and inferior occipital gyrus (Fig. 2a). A comparison of deactivation in the two groups showed lesser deactivation of the bilateral PreCu in the ε4 carriers (Fig. 2b). Additionally, we observed that the postcentral gyrus, precentral gyrus, inferior parietal lobule, and inferior occipital gyrus were significantly less active in carriers (AlphaSim-corrected, $P < 0.05$).

Relationship Between Thickness and Precuneus Deactivation

Going over the results presented above, we noted that the PreCu.R is a region where *APOE* ε4 carriers showed a simultaneous thickness reduction and an encoding-related deactivation abnormality (Fig. 3a). Differences in task-positive activations did not overlap with any structural differences. We therefore examined the correlations between task-related deactivation (PreCu.L and PreCu.R) and cortical thickness (IFG.R, Calcarine.L, and PreCu.R) for each group separately. Importantly, we found significant negative correlations between deactivation in the

TABLE II. Regions with significantly cortical thickness differences

Clusters	Regions	Peak MNI coordinates			Vertices	*P*-values
		x	*y*	*z*		
Left calcarine	Precuneus				442	
	Cuneus	−7	−72	18	491	0.0003
	Calcarine				101	
PreCu.R	Precuneus	5	−67	43	515	0.0001
	Posterior cingulate gyrus				86	
	IFG._orbital				318	
IFG.R	IFG._triangular	33	25	−4	26	<0.0001
	Insula				119	

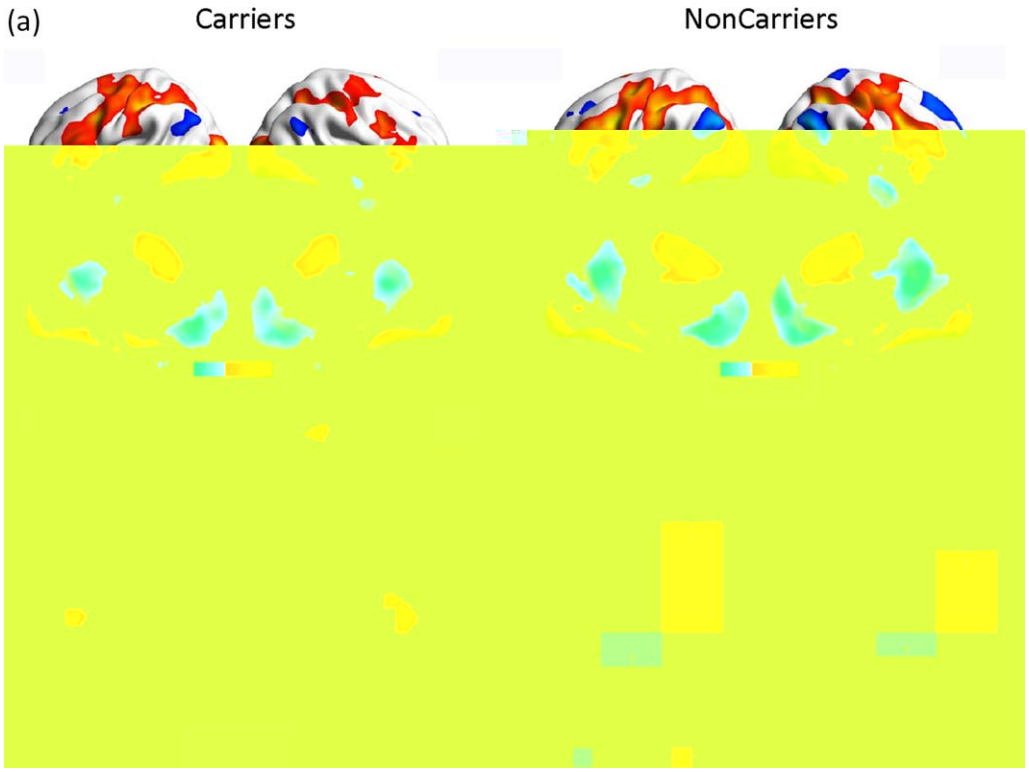

Figure 2.

The effects of *APOE* on memory-related brain activity changes. (a) Memory-induced activation and deactivation patterns in carriers and non-carriers (FDR-corrected, $q < 0.05$). Regions of brain activation are shown in red and yellow, and regions of brain deactivation are shown in blue. (b) Areas of task-induced deactivation demonstrating a significant group difference (AlphaSim-corrected, $P < 0.05$). Error bars represent the standard error of the mean parameter estimates.

PreCu.R and the cortical thickness in the IFG.R, left calcarine, and PreCu.R and between PreCu.L activation and IFG.R thickness in non-carriers. However, we found no such significant correlations in carriers (Table III).

APOE ε4 Effects on Functional Connectivity

Based on the convergence across functional and structural differences, we created a PreCu.R spherical ROI from which to compute seed-based FC maps. As shown in Figure 3b, these brain regions-MPFC, PreCu/PCC, parietal cortex and medial temporal areas have positive FC with the PreCu.R (FDR-corrected, $q < 0.05$). Areas in the insula, superior temporal gyrus (STG) and inferior parietal lobule exhibited negative FC with PreCu.R (FDR-corrected, $q < 0.05$).

Several anterior regions [the ACC, superior frontal gyrus (SFG), and middle frontal gyrus (MFG)] had decreased connectivity with the PreCu.R in carriers in positive connectivity comparisons. In the negative connectivity patterns, the STG showed an increased FC with the PreCu.R in carriers compared with non-carriers (AlphaSim-corrected, $P < 0.05$, Figure 3c and Table IV).

DISCUSSION

Neurodegenerative diseases such as AD are known to cause atrophy circumscribed by intrinsic FC networks [Seeley et al., 2009]. The main objective of our present study was to determine whether the effect of *APOE* ε4, the most prominent susceptibility gene for the risk of AD, on the brain also starts at an initial targeted region or regions serving as core areas to a subsequent large-scale network(s). We demonstrated our hypothesis that the degeneration pattern in the brains of subjects with *APOE* ε4 at the preclinical stage is similar to the degenerative pattern reported for AD. More specifically, we found that the PreCu.R is pivotal for the *APOE* effect and that it exhibited reduced cortical thickness, abnormal positive activation during a memory-encoding task and decreased FC with crucial nodes of DMN and attention/executive control networks in the *APOE* ε4 allele carriers compared with non-carriers. These findings, taken as a whole, seem to suggest that the damage pattern of *APOE* ε4 allele is precuneus-based.

Our approach in the current study is that of a selective degeneration hypothesis based on the atrophic region

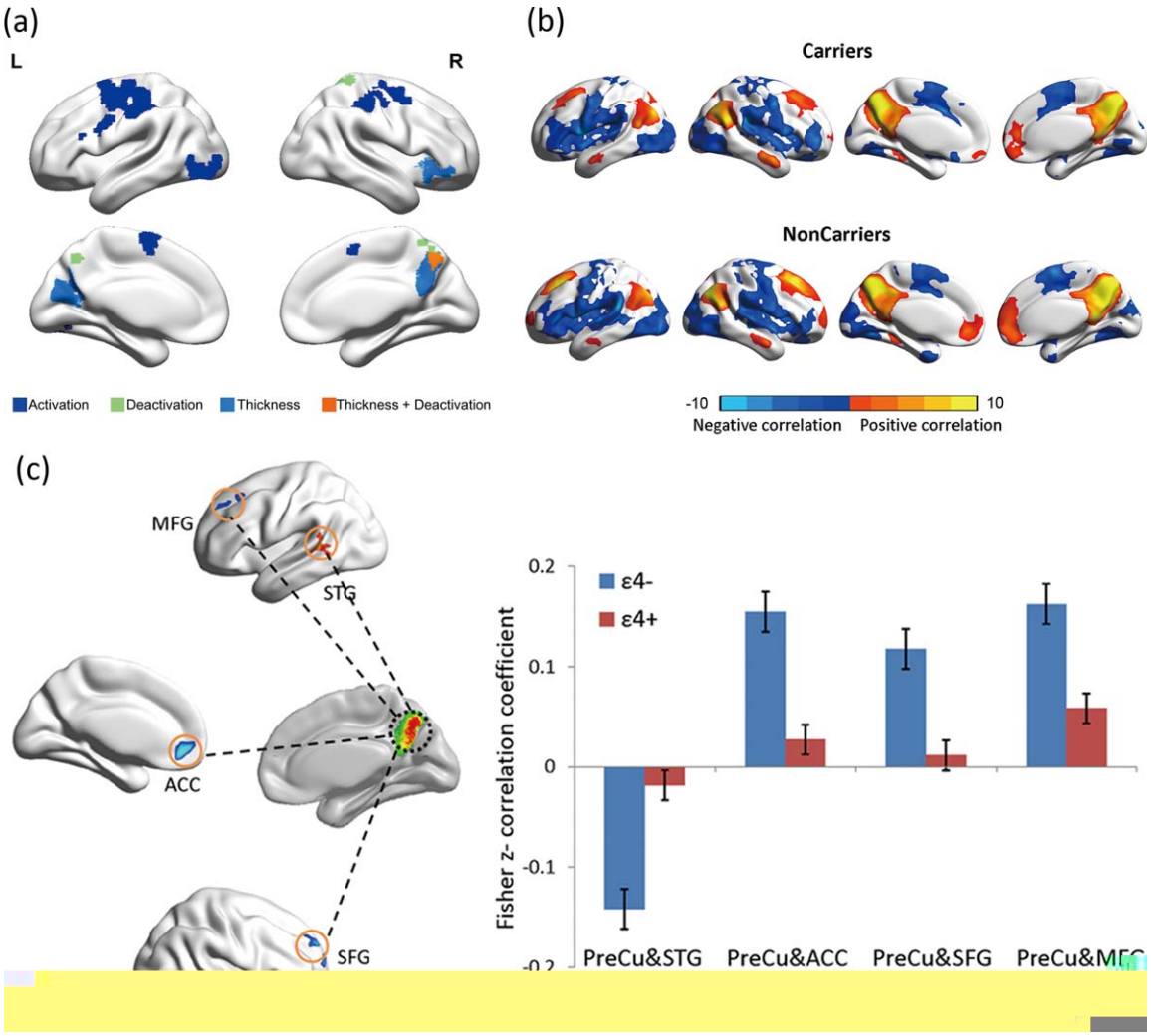

Figure 3.

Connectivity differences derived from thickness- and activation-specific seed convergence in the right precuneus. (a) Patterns of gray matter atrophy and episodic memory activation and deactivation deficits in carriers and their overlap. Brain regions coloured in dark blue and green exhibit significant group differences in activation and deactivation during memory encoding between carriers and non-carriers. Regions coloured in light blue have a significantly lower cortical thickness in carriers (FDR-corrected, $q < 0.05$). The PreCu.R area coloured in orange indicates a common disrupted region. (b) Connectivity maps derived from specific thickness and memory activation seeds converge in the PreCu.R. The seed-based connectivity analyses performed within the carriers and non-carriers using resting-state fMRI data (FDR-corrected, $q < 0.05$). Regions with positive correlations are shown in red and yellow, and negative correlations are shown in blue. (c) Altered FC of the PreCu.R in cognitively normal carriers versus non-carriers. Error bars represent the standard error of the mean connectivity values. ACC: Anterior cingulate cortex; SFG: Superior frontal gyrus; MFG: Middle superior frontal gyrus; STG: Superior temporal gyrus.

identification and its subsequent negative effects on the related networks. Overall, our results were consistent with previous findings. In probable AD patients, ε4 carriers exhibited progressive atrophy in the PreCu area relative to non-carriers [Hashimoto et al., 2009]. Cognitively normal individuals with a family history of LOAD exhibited a reduced PreCu volume compared to individuals without a family history [Berti et al., 2011; Honea et al., 2011; Honea et al., 2010]. Thus, we suggest that the structural deficit of the PreCu starts at the preclinical stage before disease onset. Moreover, the PreCu is particularly vulnerable to the early deposition of amyloid [Sperling et al., 2009]. Considering the trajectory of AD biomarkers modified by the *APOE* ε4 allele [Jack et al., 2014], one could suggest that

TABLE III. Relationship between thickness and precuneus deactivation

Regional deactivation during encoding task		Regional thickness		
		IFG.R	Calcarine.L	PreCu.R
PreCu.L	Carriers	$r = -0.33$, $P = 0.196$	$r = 0.025$, $P = 0.925$	$r = -0.19$, $P = 0.463$
	Non-carriers	$r = -0.39$, $P = 0.043$	$r = -0.251$, $P = 0.207$	$r = -0.327$, $P = 0.096$
PreCu.R	Carriers	$r = -0.256$, $P = 0.322$	$r = -0.152$, $P = 0.559$	$r = -0.234$, $P = 0.367$
	Non-carriers	$r = -0.480$, $P = 0.011$	$r = -0.377$, $P = 0.05$	$r = -0.40$, $P = 0.039$

APOE may act as a proxy of underlying neuropathology and a potential neuroimaging biomarker for early AD diagnosis.

Previous fMRI findings in healthy subjects suggested a central role for the PreCu in episodic memory [Lundstrom et al., 2005; Lundstrom et al., 2003]. Episodic memory deficits are exhibited in the early stage of AD [Welsh et al., 1991]. Our results show that the ε4 allele carriers exhibit a reduced magnitude of deactivation, which was similar to the pattern observed in patients with AD [Lustig et al., 2003; Pihlajamaki and Sperling, 2009], whereas the non-carriers exhibit proper deactivation in the bilateral PreCu under the encoding phase. Consistent with our results, diminished PreCu deactivation is also present in patients with AD and mild cognitive impairments (MCI) [Pihlajamaki and Sperling, 2009]. Previous studies in line with our results support the finding that cognitively normal elderly individual carriers exhibited decreased deactivation of PreCu in episodic memory tasks compared to non-carriers [Pihlajamaki and Sperling, 2009]. In the present study, although no group differences were found in any episodic memory measures, the deactivation of PreCu.R was lower in *APOE* ε4 carriers. Moreover, our post-hoc correlation analysis found that the decreased suppression of PreCu activity correlated with better encoding task performance in ε4 carriers. This could be interpreted by a recent hypothesis proposing that prefrontal engagement and reduced DMN suppression in older adults reflected an adaptive shift in the cognitive approach to support goal-directed task performance [Turner and Spreng, 2015]. Similar to the volumetric atrophy findings in the current study and consistent with findings from previous reports [Buckner et al., 2005; Knopman et al., 2014; Langbaum et al., 2010; Seeley et al., 2009], our task activation results also support the finding that one of the key areas affected by the *APOE* ε4 allele is the PreCu. Furthermore, we found negative correlations between deactivation in the PreCu and cortical thickness in non-carriers but not in ε4 carriers. This may indicate that the relationship between structure and function is less tightly coupled in ε4 carriers, which is a similar phenotype to that of AD patients [Delbeuck et al., 2007; Delbeuck et al., 2003].

Further, we found that the networks that are linked to the *APOE* ε4 allele and seeded at the PreCu were the DMN and the attention/executive control network. It has been documented that the PreCu is an important region in the DMN [Fransson and Marrelec, 2008]. Studies have also shown that the signals in the DMN and the attention/executive control network are antagonistic [Sridharan et al., 2008], which coincides with our results that the PreCu.R-based connectivity analyses revealed positive correlations in DMN and negative correlations in the attention/executive control network. Moreover, the present results further support the finding that the FC between the PreCu and some major nodes in the DMN and the attention/executive control network involving the ACC, SFG, MFG, and STG is decreased in ε4 carriers compared with non-carriers. This is consistent with another study that found that reduced FC of the PreCu with the left hippocampus/parahippocampus and middle temporal cortex existed in cognitively normal ε4 carriers [Sheline et al., 2010a]. Additionally, another report found diminished FC of the PreCu with the left thalamus [Zhou et al., 2013] in AD patients compared to healthy controls. A previous study also demonstrated that cognitively normal elderly individuals with amyloid deposition showed decreased connectivity between the PreCu and ACC compared to participants without amyloid deposition [Sheline et al., 2010b]. Pulling all of these findings together, we reiterate that the *APOE* ε4 allele not only disrupted the structure and function of some specific brain regions, primarily the PreCu, but also affected the whole network and weakened the relationship between the key region and networks. It is plausible that the effect of the ε4 allele progresses from its initial targeted regions to large-scale networks with crucial functions.

Extensive evidence indicates that the hippocampus is involved in episodic memory [Nellessen et al., 2015; Sexton et al., 2010], and that the hippocampus is atrophied and hypometabolic in patients with AD and MCI [La Joie et al., 2012; La Joie et al., 2014; Schroeter and Neumann, 2011]. We did not, as in an early report [Protas et al., 2013], find any structural or functional difference in this region between the ε4 carriers and non-carriers. It is worth noting that both our study and that of Protas et al. used cognitively healthy subjects characterized with the ε4 status or the gene dose and that the damage to the PreCu occurs earlier, a potential preclinical manifestation of the

APOE ε4 allele. Additional longitudinal studies are needed to verify the mechanism of the effect of *APOE* ε4 allele on brain degeneration.

This study had several limitations. First, our study was cross-sectional and the sample size was relatively small. A larger longitudinal dataset of ageing individuals is needed to verify the current results. It would be intriguing to evaluate the degeneration sequence on local cortical morphology and its spread over functional networks. Moreover, while the present study revealed evidence that the memory performance of *APOE* ε4 carriers seems to reflect the disruption of targeted functional patterns from structural atrophy and functional activity in cognitively normal elderly people, more robust assessments of different cognitive and age stages are warranted to more comprehensively understand degeneration-related mechanisms. Therefore, caution should be exercised when extrapolating our findings across the entire life span. Third, participants of different social classes or with different levels of educational achievement may exhibit different effects, which should be noted and applied in our future work. Fourth, additional studies should consider the effects of noisier data and the thinner cortical thickness in ε4 carriers to elucidate the loose coupling between structure and function in genetic risk carriers.

In conclusion, the present study emphasizes the preclinical effects of *APOE* ε4 in pivotal brain regions and connectivity patterns. The PreCu, which serves a central role, is not only a core brain region in AD and MCI [Drzezga et al., 2008; Ikonomovic et al., 2011; Langbaum et al., 2009] at the later stages of the diseases but also a vulnerable region at the early asymptomatic stage as a major node of the disease's neural network, DMN [Simic et al., 2014]. The precuneus-based degeneration patterns could help to understand the neural pathological lesions present in in patients with preclinical AD and could facilitate early network-based diagnosis and surveillance.

ACKNOWLEDGMENTS

The authors thank all the volunteers and patients for their participation in the study and anonymous reviewers for their insightful comments and suggestions.

REFERENCES

Barnes LL, Arvanitakis Z, Yu L, Kelly J, De Jager PL, Bennett DA (2013): Apolipoprotein E and change in episodic memory in blacks and whites. Neuroepidemiology 40:211–219.

Berti V, Mosconi L, Glodzik L, Li Y, Murray J, De Santi S, Pupi A, Tsui W, De Leon MJ (2011): Structural brain changes in normal individuals with a maternal history of Alzheimer's. Neurobiol Aging 32:2325 e17–2326.

Buckner RL, Snyder AZ, Shannon BJ, LaRossa G, Sachs R, Fotenos AF, Sheline YI, Klunk WE, Mathis CA, Morris JC, Mintun MA (2005): Molecular, structural, and functional characterization of Alzheimer's disease: Evidence for a relationship between default activity, amyloid, and memory. J Neurosci 25: 7709–7717.

Buckner RL, Sepulcre J, Talukdar T, Krienen FM, Liu H, Hedden T, Andrews-Hanna JR, Sperling RA, Johnson KA (2009): Cortical hubs revealed by intrinsic functional connectivity: Mapping, assessment of stability, and relation to Alzheimer's disease. J Neurosci 29:1860–1873.

Chen K, Reiman EM, Alexander GE, Caselli RJ, Gerkin R, Bandy D, Domb A, Osborne D, Fox N, Crum WR, Saunders AM, Hardy J (2007): Correlations between apolipoprotein E epsilon4 gene dose and whole brain atrophy rates. Am J Psychiatry 164: 916–921.

Chen Y, Liu Z, Zhang J, Xu K, Zhang S, Wei D, Zhang Z (2014): Altered brain activation patterns under different working memory loads in patients with type 2 diabetes. Diabetes Care 37:3157–3163.

Chen Y, Chen K, Zhang J, Li X, Shu N, Wang J, Zhang Z, Reiman EM (2015): Disrupted functional and structural networks in cognitively normal elderly subjects with the APOE varepsilon4 allele. Neuropsychopharmacology 40:1181–1191.

Chung MK, Worsley KJ, Robbins S, Paus T, Taylor J, Giedd JN, Rapoport JL, Evans AC (2003): Deformation-based surface morphometry applied to gray matter deformation. NeuroImage 18:198–213.

Coon KD, Myers AJ, Craig DW, Webster JA, Pearson JV, Lince DH, Zismann VL, Beach TG, Leung D, Bryden L, Halperin RF, Marlowe L, Kaleem M, Walker DG, Ravid R, Heward CB, Rogers J, Papassotiropoulos A, Reiman EM, Hardy J, Stephan DA (2007): A high-density whole-genome association study reveals that APOE is the major susceptibility gene for sporadic late-onset Alzheimer's disease. J Clin Psychiatry 68:613–618.

Damoiseaux JS, Seeley WW, Zhou J, Shirer WR, Coppola G, Karydas A, Rosen HJ, Miller BL, Kramer JH, Greicius MD, Alzheimer's Disease Neuroimaging, I. (2012): Gender modulates the APOE epsilon4 effect in healthy older adults: Convergent evidence from functional brain connectivity and spinal fluid tau levels. J Neurosci 32:8254–8262.

Delbeuck X, Van der Linden M, Collette F (2003): Alzheimer's disease as a disconnection syndrome? Neuropsychol Rev 13:79–92.

Delbeuck X, Collette F, Van der Linden M (2007): Is Alzheimer's disease a disconnection syndrome? Evidence from a crossmodal audio-visual illusory experiment. Neuropsychologia 45: 3315–3323.

Donix M, Burggren AC, Suthana NA, Siddarth P, Ekstrom AD, Krupa AK, Jones M, Rao A, Martin-Harris L, Ercoli LM, Miller KJ, Small GW, Bookheimer SY (2010): Longitudinal changes in medial temporal cortical thickness in normal subjects with the APOE-4 polymorphism. Neuroimage 53:37–43.

Drzezga A, Grimmer T, Henriksen G, Stangier I, Perneczky R, Diehl-Schmid J, Mathis CA, Klunk WE, Price J, DeKosky S (2008): Imaging of amyloid plaques and cerebral glucose metabolism in semantic dementia and Alzheimer's disease. Neuroimage 39:619–633.

Felsky D, Voineskos AN, Lerch JP, Nazeri A, Shaikh SA, Rajji TK, Mulsant BH, Kennedy JL (2012): Myelin-associated glycoprotein gene and brain morphometry in schizophrenia. Front Psychiatry 3:40.

Ferri CP, Prince M, Brayne C, Brodaty H, Fratiglioni L, Ganguli M, Hall K, Hasegawa K, Hendrie H, Huang Y, Jorm A, Mathers C, Menezes PR, Rimmer E, Scazufca M (2005): Global prevalence of dementia: A Delphi consensus study. Lancet 366: 2112–2117.

Fransson P, Marrelec G (2008): The precuneus/posterior cingulate cortex plays a pivotal role in the default mode network: Evidence from a partial correlation network analysis. Neuroimage 42:1178–1184.

Gong G, He Y, Chen ZJ, Evans AC (2012): Convergence and divergence of thickness correlations with diffusion connections across the human cerebral cortex. NeuroImage 59:1239–1248.

Goveas JS, Xie C, Chen G, Li W, Ward BD, Franczak MB, Jones JL, Antuono PG, Li SJ (2013): Functional network endophenotypes unravel the effects of apolipoprotein E epsilon 4 in middle-aged adults. PLoS One 8:12.

Hashimoto R, Hirata Y, Asada T, Yamashita F, Nemoto K, Mori T, Moriguchi Y, Kunugi H, Arima K, Ohnishi T (2009): Effect of the brain-derived neurotrophic factor and the apolipoprotein E polymorphisms on disease progression in preclinical Alzheimer's disease. Genes, Brain Behav 8:43–52.

Honea RA, Swerdlow RH, Vidoni ED, Goodwin J, Burns JM (2010): Reduced gray matter volume in normal adults with a maternal family history of Alzheimer disease. Neurology 74: 113–120.

Honea RA, Swerdlow RH, Vidoni ED, Burns JM (2011): Progressive regional atrophy in normal adults with a maternal history of Alzheimer disease. Neurology 76:822–829.

Ikonomovic MD, Klunk WE, Abrahamson EE, Wuu J, Mathis CA, Scheff SW, Mufson EJ, DeKosky ST (2011): Precuneus amyloid burden is associated with reduced cholinergic activity in Alzheimer disease. Neurology 77:39–47.

Jack CR, Jr, Wiste HJ, Weigand SD, Rocca WA, Knopman DS, Mielke MM, Lowe VJ, Senjem ML, Gunter JL, Preboske GM, Pankratz VS, Vemuri P, Petersen RC (2014): Age-specific population frequencies of cerebral beta-amyloidosis and neurodegeneration among people with normal cognitive function aged 50-89 years: A cross-sectional study. Lancet Neurol 13:997–1005.

Kabani N, Le Goualher G, MacDonald D, Evans AC (2001): Measurement of cortical thickness using an automated 3-D algorithm: A validation study. NeuroImage 13:375–380.

Kim JS, Singh V, Lee JK, Lerch J, Ad-Dab'bagh Y, MacDonald D, Lee JM, Kim SI, Evans AC (2005): Automated 3-D extraction and evaluation of the inner and outer cortical surfaces using a Laplacian map and partial volume effect classification. NeuroImage 27:210–221.

Klunk WE, Engler H, Nordberg A, Wang Y, Blomqvist G, Holt DP, Bergstrom M, Savitcheva I, Huang GF, Estrada S, Ausen B, Debnath ML, Barletta J, Price JC, Sandell J, Lopresti BJ, Wall A, Koivisto P, Antoni G, Mathis CA, Langstrom B (2004): Imaging brain amyloid in Alzheimer's disease with Pittsburgh Compound-B. Ann Neurol 55:306–319.

Knopman DS, Jack CR, Wiste HJ, Lundt ES, Weigand SD, Vemuri P, Lowe VJ, Kantarci K, Gunter JL, Senjem ML, Mielke MM, Roberts RO, Boeve BF, Petersen RC (2014): 18F-fluorodeoxyglucose positron emission tomography, aging, and apolipoprotein E genotype in cognitively normal persons. Neurobiol Aging 35:2096–2106.

La Joie R, Perrotin A, Barre L, Hommet C, Mezenge F, Ibazizene M, Camus V, Abbas A, Landeau B, Guilloteau D, de La Sayette V, Eustache F, Desgranges B, Chetelat G (2012): Region-specific hierarchy between atrophy, hypometabolism, and beta-amyloid (Abeta) load in Alzheimer's disease dementia. J Neurosci 32:16265–16273.

La Joie R, Landeau B, Perrotin A, Bejanin A, Egret S, Pélerin A, Mézenge F, Belliard S, de La Sayette V, Eustache F, Desgranges B, Chételat G (2014): Intrinsic connectivity identifies the hippocampus as a main crossroad between Alzheimer's and semantic dementia-targeted networks. Neuron 81:1417–1428.

Langbaum JBS, Chen K, Lee W, Reschke C, Bandy D, Fleisher AS, Alexander GE, Foster NL, Weiner MW, Koeppe RA, Jagust WJ, Reiman EM (2009): Categorical and correlational analyses of baseline fluorodeoxyglucose positron emission tomography images from the Alzheimer's disease neuroimaging initiative (ADNI). Neuroimage 45:1107–1116.

Langbaum JBS, Chen K, Caselli RJ, Lee W, Reschke C, Bandy D, Alexander GE, Burns CM, Kaszniak AW, Reeder SA, Corneveaux JJ, Allen AN, Pruzin J, Huentelman MJ, Fleisher AS, Reiman EM (2010): Hypometabolism in Alzheimer-affected brain regions in cognitively healthy latino individuals carrying the apolipoprotein E ε4 allele. Arch Neurol 67:

Lerch JP, Evans AC (2005): Cortical thickness analysis examined through power analysis and a population simulation. NeuroImage 24:163–173.

Lundstrom BN, Petersson KM, Andersson J, Johansson M, Fransson P, Ingvar M (2003): Isolating the retrieval of imagined pictures during episodic memory: Activation of the left precuneus and left prefrontal cortex. Neuroimage 20: 1934–1943.

Lundstrom BN, Ingvar M, Petersson KM (2005): The role of precuneus and left inferior frontal cortex during source memory episodic retrieval. Neuroimage 27:824–834.

Lustig C, Snyder AZ, Bhakta M, O'Brien KC, McAvoy M, Raichle ME, Morris JC, Buckner RL (2003): Functional deactivations: Change with age and dementia of the Alzheimer type. Proc Natl Acad Sci U S A 100:14504–14509.

Lyttelton OC, Karama S, Ad-Dab'bagh Y, Zatorre RJ, Carbonell F, Worsley K, Evans AC (2009): Positional and surface area asymmetry of the human cerebral cortex. NeuroImage 46:895–903.

Machulda MM (2011): Effect of APOE ε4 status on intrinsic network connectivity in cognitively normal elderly subjects. Arch Neurol 68:1131.

McKiernan KA, Kaufman JN, Kucera-Thompson J, Binder JR (2003): A parametric manipulation of factors affecting task-induced deactivation in functional neuroimaging. J Cogn Neurosci 15:394–408.

Murray ME, Graff-Radford NR, Ross OA, Petersen RC, Duara R, Dickson DW (2011): Neuropathologically defined subtypes of Alzheimer's disease with distinct clinical characteristics: A retrospective study. Lancet Neurol 10:785–796.

Nellessen N, Rottschy C, Eickhoff SB, Ketteler ST, Kuhn H, Shah NJ, Schulz JB, Reske M, Reetz K (2015): Specific and disease stage-dependent episodic memory-related brain activation patterns in Alzheimer's disease: A coordinate-based meta-analysis. Brain Struct Funct 220:1555–1571.

Nichols LM, Masdeu JC, Mattay VS, Kohn P, Emery M, Sambataro F, Kolachana B, Elvevag B, Kippenhan S, Weinberger DR, Berman KF (2012): Interactive effect of apolipoprotein e genotype and age on hippocampal activation during memory processing in healthy adults. Arch Gen Psychiatry 69:804–813.

Pihlajamaki M, Sperling RA (2009): Functional MRI assessment of task-induced deactivation of the default mode network in Alzheimer's disease and at-risk older individuals. Behav Neurol 21:77–91.

Pihlajamaki M, DePeau KM, Blacker D, Sperling RA (2008): Impaired medial temporal repetition suppression is related to failure of parietal deactivation in Alzheimer disease. Am J Geriatr Psychiatry 16:283–292.

Protas HD, Chen K, Langbaum JBS, Fleisher AS, Alexander GE, Lee W, Bandy D, de Leon MJ, Mosconi L, Buckley S, Truran-Sacrey D, Schuff N, Weiner MW, Caselli RJ, Reiman EM (2013): Posterior cingulate glucose metabolism, hippocampal glucose metabolism, and hippocampal volume in cognitively normal, late-middle-aged persons at 3 levels of genetic risk for Alzheimer disease. JAMA Neurol 70:320.

Purcell S, Neale B, Todd-Brown K, Thomas L, Ferreira MA, Bender D, Maller J, Sklar P, De Bakker PI, Daly MJ (2007): PLINK: A tool set for whole-genome association and population-based linkage analyses. Am J Hum Genet 81: 559–575.

Reinvang I, Espeseth T, Westlye LT (2013): APOE-related biomarker profiles in non-pathological aging and early phases of Alzheimer's disease. Neurosci Biobehav Rev 37:1322–1335.

Schroeter ML, Neumann J (2011): Combined imaging markers dissociate Alzheimer's disease and frontotemporal lobar degeneration—An ALE meta-analysis. Front Aging Neurosci 3:10.

Seeley WW, Crawford RK, Zhou J, Miller BL, Greicius MD (2009): Neurodegenerative diseases target large-scale human brain networks. Neuron 62:42–52.

Sexton CE, Mackay CE, Lonie JA, Bastin ME, Terriere E, O'Carroll RE, Ebmeier KP (2010): MRI correlates of episodic memory in Alzheimer's disease, mild cognitive impairment, and healthy aging. Psychiatry Res 184:57–62.

Shaw P, Lerch JP, Pruessner JC, Taylor KN, Rose AB, Greenstein D, Clasen L, Evans A, Rapoport JL, Giedd JN (2007): Cortical morphology in children and adolescents with different apolipoprotein E gene polymorphisms: An observational study. Lancet Neurol 6:494–500.

Sheline YI, Morris JC, Snyder AZ, Price JL, Yan Z, D'Angelo G, Liu C, Dixit S, Benzinger T, Fagan A, Goate A, Mintun MA (2010a): APOE4 allele disrupts resting state fMRI connectivity in the absence of amyloid plaques or decreased CSF Abeta42. J Neurosci 30:17035–17040.

Sheline YI, Raichle ME, Snyder AZ, Morris JC, Head D, Wang S, Mintun MA (2010b): Amyloid plaques disrupt resting state default mode network connectivity in cognitively normal elderly. Biol Psychiatry 67:584–587.

Simic G, Babic M, Borovecki F, Hof PR (2014): Early failure of the default-mode network and the pathogenesis of Alzheimer's disease. CNS Neurosci Therapeutics 20:692–698.

Sled JG, Zijdenbos AP, Evans AC (1998): A nonparametric method for automatic correction of intensity nonuniformity in MRI data. Med Imaging, IEEE Trans 17:87–97.

Sperling RA, Laviolette PS, O'Keefe K, O'Brien J, Rentz DM, Pihlajamaki M, Marshall G, Hyman BT, Selkoe DJ, Hedden T, Buckner RL, Becker JA, Johnson KA (2009): Amyloid deposition is associated with impaired default network function in older persons without dementia. Neuron 63:178–188.

Sridharan D, Levitin DJ, Menon V (2008): A critical role for the right fronto-insular cortex in switching between central-executive and default-mode networks. Proc Natl Acad Sci U S A 105:12569–12574.

Taylor JE, Adler RJ (2003): Euler characteristics for Gaussian fields on manifolds. Ann Prob 533–563.

Tohka J, Zijdenbos A, Evans A (2004): Fast and robust parameter estimation for statistical partial volume models in brain MRI. NeuroImage 23:84–97.

Turner GR, Spreng RN (2015): Prefrontal engagement and reduced default network suppression co-occur and are dynamically coupled in older adults: The default-executive coupling hypothesis of aging. J Cogn Neurosci 27:2462–2476.

Wang L, Li H, Liang Y, Zhang J, Li X, Shu N, Wang YY, Zhang Z (2013): Amnestic mild cognitive impairment: Topological reorganization of the default-mode network. Radiology 268: 501–514.

Welsh K, Butters N, Hughes J, Mohs R, Heyman A (1991): Detection of abnormal memory decline in mild cases of Alzheimer's disease using CERAD neuropsychological measures. Arch Neurol 48:278–281.

Zhou J, Gennatas ED, Kramer JH, Miller BL, Seeley WW (2012): Predicting regional neurodegeneration from the healthy brain functional connectome. Neuron 73:1216–1227.

Zhou B, Liu Y, Zhang Z, An N, Yao H, Wang P, Wang L, Zhang X, Jiang T (2013): Impaired functional connectivity of the thalamus in Alzheimer's disease and mild cognitive impairment: A resting-state fMRI study. Curr Alzheimer Res 10:754–766.